Article

Not peer-reviewed version

Dynamics of Built-Up Areas and Loss of Vegetation in Secondary Towns: Case Study of Sarh Town in Chad, Central Africa

François Teadoum Naringué *, N'Dilbé Tob-Ro, Melone Like Sorsy, Julien Komivi Sodjinè Aboudou, Asrom Blondel Mgang-yo, Bourdannet Patouki Sing-Non, Altolnan Parfait Tombar, Follygan Hetcheli

Posted Date: 10 December 2024

doi: 10.20944/preprints202412.0754.v1

Keywords: built-up areas; vegetation; urban sprawl; secondary towns; urbanisation

 doi:10.20944/preprints202412.0754.v1

Article

Dynamics of Built-Up Areas and Loss of Vegetation in Secondary Towns: Case Study of Sarh Town in Chad, Central Africa

François Teadoum Naringué [1,2,*], N'Dilbé Tob-Ro [3], Melone Like Sorsy [2], Julien Komivi Sodjinè Aboudou [4], Asrom Blondel Mgang-yo [1], Bourdannet Patouki Sing-Non [1], Altolnan Parfait Tombar [1] and Follygan Hetcheli [2]

[1] Regional Center of Excellence on Sustainable Cities in Africa (CERViDA-DOUNEDON), University of Lome, Lome 01 BP 1515, Togo
[2] Research Laboratory on Spaces, Exchanges and Human Security, University of Lome, Lome 01 BP1515, Togo
[3] Adam Barka University of Abeche, N'Djamena, BP 5539, Chad
* Correspondence: francois.teadoumnaringue@cervida-togo.org or teadoumnaringue@gmail.com

Abstract: The expansion of secondary towns in Africa, although less rapid than that of capital cities, poses significant challenges for environmental sustainability. Sarh town (Chad) is an example of this urbanisation phenomenon, which has led to a significant loss of vegetation. This research aims to analyse the dynamics of land use, focusing on the expansion of built-up areas and the loss of vegetation. The methodology used includes the analysis of Landsat images from 1994, 2003, 2013 and 2022, supplemented by field data, statistical analysis, interviews and documentary analysis. The results show that the built-up area, estimated at 806 hectares in 1994, reached 2,603 hectares in 2022, representing an annual increase of 4.1%. Moreover, the area of vegetation decreased from 759 hectares to 231 hectares, a reduction of 69%. In addition, there is a strong negative correlation (r =-0.93) between the expansion of built-up areas and the loss of vegetation. On average, the annual growth of built-up areas (4.1%) exceeds that of the population (3.33%). Field surveys reveal that this situation is due to a preference for more spacious housing, inadequate land management and limited resources for vegetation rehabilitation. These results highlight the need to adopt effective planning tools to ensure sustainable land use.

Keywords: built-up areas; vegetation; urban sprawl; secondary towns; urbanisation

1. Introduction

Rapid urban expansion and its implications for vegetation dynamics are major concerns for the 21st century, particularly in developing countries [1]. Globally, trends show a rapid increase in urbanisation, leading to urban sprawl and massive land-use change [2–4]. If left unchecked, such rapid growth could have detrimental effects on the environment, seriously threatening green spaces [5,6]. However, vegetation is part of the composite urban ecosystem, providing ecological services that are essential to the construction of the urban ecological environment [7].

In sub-Saharan Africa, rapid urbanisation is a major challenge for sustainable development, leading to significant transformations of urban landscapes and surrounding ecosystems [8]. This urban expansion often results in the occupation of peripheral areas without respect for town planning regulations [9–11], posing a serious challenge for environmental management in urban areas [12,13]. This phenomenon is particularly prominent in small towns or secondary cities with fewer than 500,000 inhabitants, where the majority of the world's city dwellers live [14]. According to Tripathi and Mitra [15], small towns play a crucial role in current economic development. Maru et al. [16] noted that these cities lack specific data on urban problems, as does the necessary analysis for spatial

 doi:10.20944/preprints202412.0754.v1

planners and policymakers. The dynamics of built-up areas and their implications for urban vegetation remain poorly studied.

Understanding urban dynamics and their consequences in sub-Saharan Africa has become an important research topic [17]. Many studies have demonstrated that the remote sensing and spatial measurements can be used to quantify and compare urban growth, as well as its shape, pattern and spatiotemporal structure [17–22]. Earlier work, such as that by Blakime et al. [24], explored the dynamics of built-up areas through the analysis of satellite images, highlighting changes in land use in Greater Lomé in Togo. Furthermore, studies have revealed a negative correlation between the expansion of built-up areas and the loss of vegetation, highlighting the direct impact of urbanisation on local ecosystems [25]. As far as capital cities are concerned, research by Abo-El-Wafa et al. [26] on Addis Ababa, by Nshimiyimana et al. [27] on Kigali and by Seth et al. [28] on Dar El Salam, Accra and Luanda has demonstrated an increase in built-up areas accompanied by a reduction in vegetated areas.

However, despite these significant contributions, there are gaps in the literature. In general, scientific studies on urban life are carried out in metropolises, thus failing to represent its full diversity [29]. Few studies have focused on small African cities, leaving a gap in our understanding of the specific features of their urban development. For example, the works of Awuh et al. [30] on Calabar in Nigeria, Takam Tiamgne et al. [31] on Solwezi in Zambia, Dechaicha and Alkama [32] on Bou Saâda in Algeria and Takyi et al. [33] on Kwabre East in Ghana, although important, present certain shortcomings. These shortcomings concern mainly the methodological approach, particularly cross-validation with existing field data and cadastral plans, the integration of demographic data and interviews, and statistics in the analysis of urban dynamics. Moreover, very few of these studies focus on spatiotemporal changes in the dynamics of built-up areas and their implications for secondary towns in Central Africa.

Sarh town, located south of Chad in the Sudanian zone, is characterised by its abundant vegetation, which has often been destroyed by urban development, depriving the town of its natural spaces, which were once intended to refresh the urban environment. According to Teadoum Naringué et al. [13], Sarh is one of the Chadian urban centers whose spatial growth exceeds the limits of the official spatial planning tool, particularly the reference urban plan (RUP). Its spatial expansion is the result of a preference for single-family homes and more spacious accommodations, as well as the conversion of certain rural areas into urban zones. Although population growth does not keep pace with that of capital, it requires access to land that is not effectively managed by local authorities. This situation has led to an alarming loss of vegetation, which is essential for cooling the urban environment and providing the ecological functions needed to maintain ecosystems. As a result, the dynamics of built-up areas and the management of natural resources are becoming central issues for urban planning and sustainable land use in Sarh. The literature reveals that uncontrolled urban expansion leads to an increase in spontaneous occupation, thereby aggravating land speculation and environmental problems [34].

The research question that emerges from this issue is as follows: how do the dynamics of built-up areas in Sarh affect vegetation, and what are the challenges associated with sustainable land-use planning in this context? This issue is crucial, as it affects not only the quality of life of local residents but also the sustainability of natural resources in a rapidly changing environment. Recurrent flooding, exacerbated by uncontrolled urbanisation, illustrates the dramatic consequences of this dynamic, as highlighted [35].

The production of scientific knowledge on the dynamics of land occupation and use could be an important step in informing town managers and other urban players about its growth and the spatial transformations that accompany it. Few studies have explored the dynamics of built-up areas and their impact on vegetation in Sarh town. It is therefore essential to fill this gap in academic research to make a significant contribution to sustainable land-use planning and urban development.

This research aims to analyse the dynamics of land use, focusing on the expansion of built-up areas and the loss of vegetation between 1994 and 2022. Specifically, the aims of this study are to (1) quantify the dynamics of built-up areas and the loss of vegetation in Sarh town; (2) measure the

 doi:10.20944/preprints202412.0754.v1

degree of expansion of built-up areas in relation to population growth in Sarh town; and (3) identify development and planning issues for sustainable land use. The results of this research will be used to support urban land-use planning in Chad and other developing countries.

2. Materials and Methods

2.1. Materials

2.1.1. Study Area

This study was carried out in Sarh town, the capital of the province of Moyen-Chari, and the Department of Barh-Kôh in Chad, which is located between 09° and 10° North latitude and 18° and 19° East longitude [36]. Sarh town is bounded to the north and east by the municipality of Hellibongo, to the south by the municipality of Banda, and to the west by the municipality of Balimba [13]. It is subdivided into 6 districts and 30 neighbourhoods, with a population of 97,224 in 2009 [37] and an estimated total population of 180,000 in 2018 [38]. It covers an area of 38.04 km², or 0.003% of the national territory [13], and is the 4th largest city in Chad in terms of population, after N'Djamèna, Moundou and Abéché [38]. The location of Sarh town is shown in Figure 1 below.

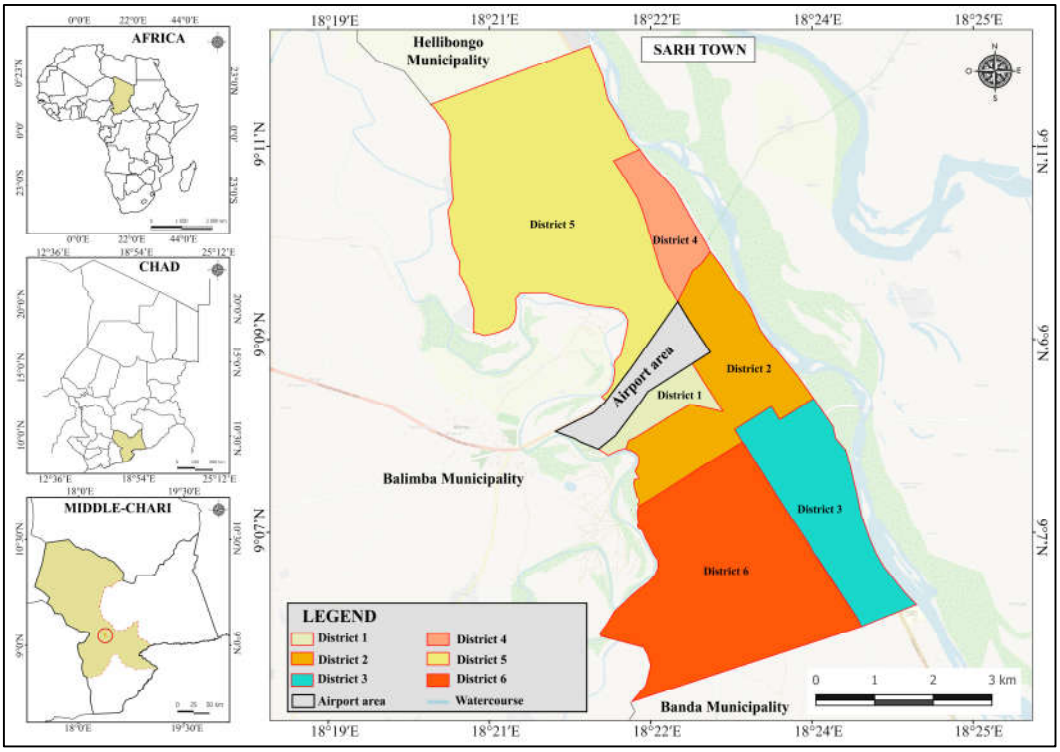

Figure 1. Location of Sarh Town.

2.1.2. Acquisition of Landsat Satellite Data

The data used in this study come from Landsat sensors. These are four satellite images from different dates. The satellite images for 1994 and 2003 were acquired by the Landsat 5 Thematic Mapper (TM) and Landsat 7 Thematic Mapper (TM), respectively, and those for 2013 and 2022 were acquired by the Landsat 8 Operational Land Imager-Thermal Infrared Sensor (OLI-TIRS). Numerous studies on urban land consumption analysis have been carried out using Landsat images [2,39–44]. These images were downloaded from the United States Geological Survey (USGS) platform at the following address: https://earthexplorer.usgs.gov/. They are referenced to the WGS 1984 global geodetic system and reprojected onto the WGS84 UTM zone 33 N ellipsoid. The acquisition format is essentially GEOTIFF and its metadata (txt, json, xlm, enp, jpg).

 doi:10.20944/preprints202412.0754.v1

According to Whitcraft et al. [45], clouds represent a major challenge for remote sensing. To minimise this impact, images were acquired between November and April, a period corresponding to the dry season in the study environment. Using images during the dry season reduces the bias introduced into the results by seasonal variations and the impact of cloud cover [2,46,47]. This choice made it possible to obtain images with very low cloud cover (10%). Level 2 products (surface reflectance) from the Landsat 5, Landsat 7 and Landsat 8 satellites from 1994, 2003, 2013 and 2022 were selected to obtain data in which atmospheric effects and other biases were removed or reduced [48].

Landsat images were selected because of their open-source nature and good temporal, spectral, spatial and radiometric resolutions. In addition, the dates on which the satellite data were acquired were chosen to correlate them with the years of the general population and housing censuses and the dates of the sociodemographic surveys carried out in Sarh town. The years were chosen with reference to those of the general population and housing censuses, which, according to United Nations recommendations, should be carried out every 10 years [37]. The characteristics of the images collected are shown in Table 1 below.

Table 1. Characteristics of the images collected.

Years	Landsat Scenes	Sensors	Spatial resolutions	Acquisition dates	Cloud cover
1994	Landsat 5	TM	30 m	29/11/1994	-10%
2003	Landsat 7	ETM+	30 m	30/01/2003	
2013	Landsat 8	OLI-TIRS	30 m	19/12/2013	
2022	Landsat 8	OLI-TIRS	30 m	28/12/2022	

2.1.3. Acquisition of Landsat Satellite Data Auxiliary Data Acquisition

In addition to satellite data, the following ancillary data were used: the administrative boundary of Sarh town obtained from the cartography department of the National Development Research Center (CNRD), high-resolution (5 m) Google Earth Pro ortho photos recorded at various Landsat image acquisition dates (1994, 2003, 2013 and 2022), and georeferenced cadastral plans obtained from the provincial delegation for development, housing and urban planning. In addition, general census and demographic survey data obtained from the National Institute of Statistics, Economic and Demographic Studies (INSEED) were also used in this study.

2.2. Methods

2.2.1. Determination of Land Use and Land Cover (LULC) Classes

The LULC classes were defined in two stages. First, four land use and occupancy classes were defined on the basis of the four spectral indices calculated. These areas included built-up areas, vegetation, water areas and bare land (Table 2). The residential area was then categorised into three subclasses to analyse changes in the density of built-up areas in Sarh town (Table 3). This method was used in previous work by Blakime et al. [24].

Table 2. Categories of LULC.

Occupation classes	**Description**
Built-up area	Urban features such as buildings, streets and landscaped areas
Vegetation	Landscaped green areas, large trees and shrubs
Bare Land	All areas other than built-up areas, developed land and vegetation
Water area	Ponds, marshes

Table 3. Subcategories based on built-up areas.

 doi:10.20944/preprints202412.0754.v1

Occupation classes	Description
High built-up area	Areas more than 75% covered by built-up area
Medium built-up area	Areas covered by between 50% and 75% of built-up area
Low built-up area	Covered areas with less than 50% built-up area
Other classes	Vegetation, bare land and water area

2.2.2. Satellite Data Processing and Classification

For the processing and classification process, in addition to the conventional bands (B2, B3, B4, and B5) for all the Landsat family sensor collections, four spectral indices were used [49,50]. These indices are the bare soil index (BSI), the normalised difference building index (NDBI), the modified normalised difference water index (MNDWI) and the ground-adjusted vegetation index (SAVI). According to Zhao et al. [51], the integration of these indices into the classification process allows for a more comprehensive analysis of LULC, capturing key features related to vegetation, built-up areas and water areas. This technique improves the accuracy and efficiency of the classification results. All these indices vary between -1 and 1.

The bare soil index (BSI) is a numerical indicator that combines information in the blue, red, near infrared and shortwave infrared spectral bands to capture soil variations [52]. According to Ettehadi Osgouei et al. [53], this index provides a better understanding of the transformations that have taken place in the areas examined and enables more reliable results to be obtained. This index is calculated via equation (1):

$$\mathrm{BSI} = \frac{((\mathrm{Red} - \mathrm{SWIR})) - (\mathrm{NIR} - \mathrm{Blue}))}{((\mathrm{Red} - \mathrm{SWIR})) + (\mathrm{NIR} + \mathrm{Blue}))} \quad (1)$$

where Blue, Red, NIR, and SWIR are the blue, red, near infrared and shortwave infrared reflectances, respectively.

The normalised difference building index highlights urban areas with higher reflectances in the shortwave infrared (SWIR) region than in the near infrared (NIR) region [54]. A higher value represents built-up areas, a lower value represents vegetation, and a negative value represents water areas [24]. This is illustrated by the following equation (2):

$$\mathrm{NDBI} = \frac{\mathrm{SWIR} - \mathrm{NIR}}{\mathrm{SWIR} + \mathrm{NIR}} \quad (2)$$

where SWIR is the shortwave near-infrared reflectance and NIR is the near-infrared reflectance.

The modified normalised difference water index (MNDWI) uses the green and SWIR bands to enhance the characteristics of open water [24]. The MNDWI is sensitive to water masses, with higher values indicating the presence of water [50]. Compared with the NDWI, it is more suitable for enhancing and extracting water information for aquatic regions with backgrounds dominated by built-up areas because of its ability to reduce or even suppress built-up noise [55]. This index is calculated via equation (3):

$$\mathrm{MNDWI} = \frac{\mathrm{Green} - \mathrm{SWIR}}{\mathrm{Green} + \mathrm{SWIR}} \quad (3)$$

where Green represents the reflectance in the green range and SWIR represents the reflectance in the shortwave region near the infrared region.

The soil adjusted vegetation index (SAVI) is an index developed by Huete to measure plant biomass via light reflectance at red and near-infrared wavelengths [56]. This is an important index for scientists studying vegetation, as it is stable and does not vary according to soil color and moisture or saturation effects due to high-density vegetation [52]. It is determined by the following equation (4):

$$\mathrm{SAVI} = \frac{(\mathrm{NIR} - \mathrm{Red})}{(\mathrm{NIR} + \mathrm{Red} + \mathrm{L})} \times (1 + \mathrm{L}) \quad (4)$$

where L represents a correction factor for ground luminosity. To take account of soil brightness for most LULC types, the L types are defined as 0.5.

 doi:10.20944/preprints202412.0754.v1

Principal component analysis was carried out on the four spectral indices via Orfeo Toolbox 9.0.0, integrated with QGIS 3.24, to maximise the information contained in the bands and improve the discrimination of LULC classes. These indices were combined and include the bare soil index (BSI), the normalised difference building index (NDBI), the normalised difference moisture index (MNDWI) and the soil adjusted normalised difference vegetation index (SAVI) [51]. A principal component analysis was carried out for the four years considered in this study, i.e., 1994, 2003, 2013 and 2022. The results of this analysis were then used to carry out a supervised classification based on the training plots collected during the fieldwork and using Google Earth pro ortho photos and georeferenced cadastral maps for the years 1994, 2003 and 2013 (Figure 2).

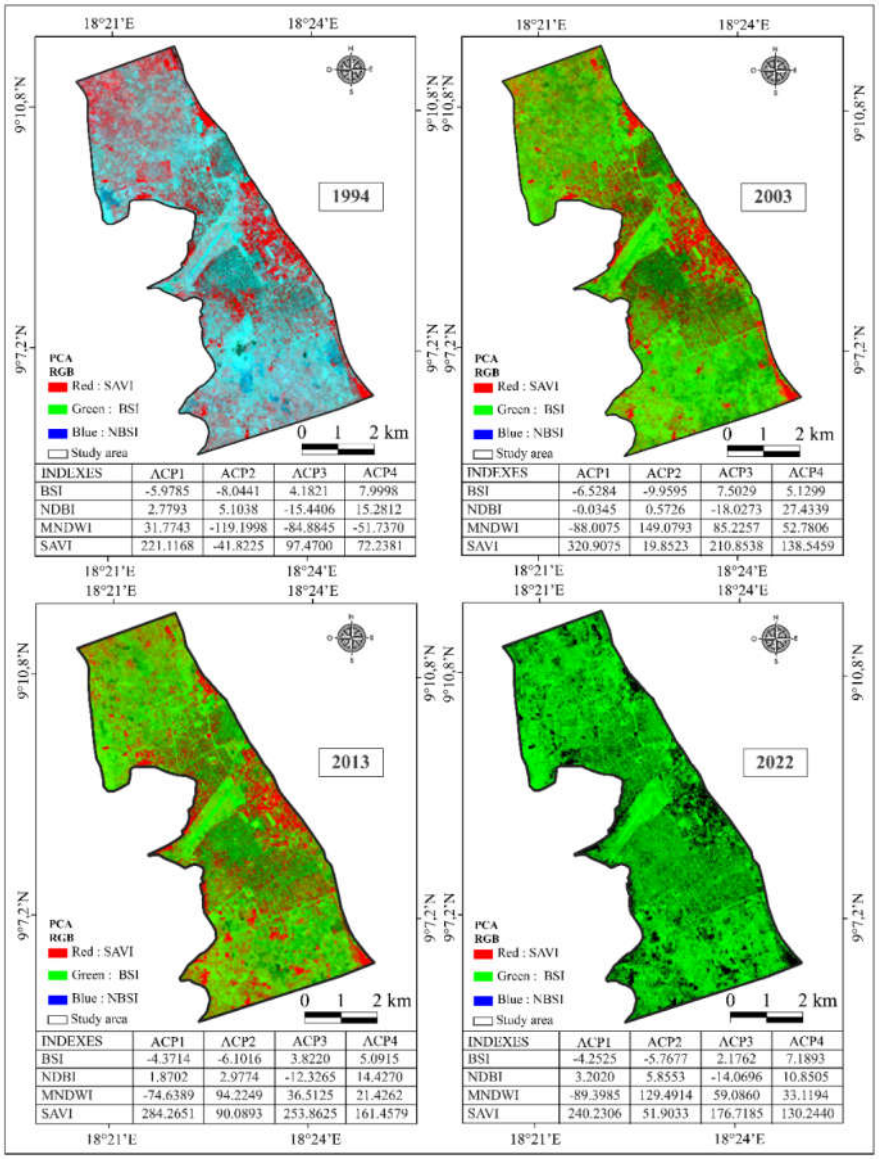

Figure 2. Results of principal component analysis.

Classification was carried out via the random forest (RF) algorithm in Orfeo Toolbox 9.0.0, which is based on a sample of 300 to 400 training plots (ROIs). The random forest algorithm is an efficient machine learning algorithm proposed by Breiman [57]. It has been widely used in previous studies for satellite image classification and geo-information processing [56–60]. This algorithm was chosen because it is an effective tool for predicting land cover [55,60]. It is generally insensitive to data noise and overfitting and is extremely useful for classifying data [60,61,63]. In addition, the RF classifier has allowed us to successfully handle high data dimensionality and generally achieves higher accuracy than other approaches, such as maximum likelihood, single decision trees and single-layer

 doi:10.20944/preprints202412.0754.v1

neural networks [61]. In addition, RF allows missing values to be estimated and several types of data analysis to be performed, including regression, classification and unsupervised learning [64].

2.2.3. Validation of the Classification Result via the Kappa Index and Overall Precision

The first validation of the classification accuracy was carried out by calculating the Kappa index and the overall accuracy using the transition matrices. The kappa index developed by Cohen is a powerful statistical measure widely used to assess the performance of a model generating presence/absence predictions [65]. It is accepted as a measure of classification accuracy for both the model and the user of the classification model [30]. The value of the kappa coefficient varies from 0 to 1, where 0 represents the lowest accuracy between the ground truth and classified images, and a value > 0.85 indicates high agreement between the two datasets [12]. An overall accuracy of 50% is poor, that between 50% and 70% is moderate, and an accuracy above 70% is considered good [19]. The overall accuracy and kappa index are expressed in equations (5) and (6):

$$\text{Kappa (K)} = \frac{\text{Po} - \text{Pe}}{1 - \text{Pe}} \quad (5)$$

Po (observed agreement) is the proportion of correct classifications (sum of true positives).
Pe (random agreement) is the proportion of agreement expected by chance.

$$\text{PG} = \frac{\sum_{=1}^{n} \text{Xii}}{\text{N}} \times 100 \quad (6)$$

where PG is the overall accuracy; Xii is the value on the diagonal of the confusion matrix representing the correct predictions for each class; and N is the sum of all the values in the confusion matrix.

2.2.4. Cross-Validation of the Classification: Overlay of the Classification with Ortho Photos from Google Earth Pro and Existing Cadastral Maps

After classification, the results were superimposed on cadastral plans and spatially referenced field data on the one hand and on Google Earth Pro ortho photos on the other hand. To do this, archives of cadastral plans and high-resolution Google Earth ortho photos were used to compare and improve the accuracy of the classification. Google Earth Pro ortho photos associated with control points (field data) have been widely used to compare and validate classification results [21,63,64]. Four Google Earth Pro ortho photo backgrounds were used, corresponding to the acquisition dates of the Landsat images (1994, 2003, 2013 and 2022). These orthoimages were recorded more or less on the same days as the Landsat images were acquired to obtain the same information on LULC. For each date, the LULC classes were superimposed on the field data, the Google Earth Pro orthophoto background, and the existing cadastral maps. The exercise was made possible by the following manipulations:

The raster image resulting from the classification was polygonized (conversion from raster mode to vector mode). This operation was carried out for each year of analysis. The vectors resulting from the polygonization were projected onto the field data, Google Earth Pro ortho photos and cadastral maps to detect any errors. The spaces corresponding to the incorrectly classified pixels were selected and reclassified to obtain the final classification result.

2.2.5. Change Detection

The maps classified between two years were compared via the multivariate alteration detector (MAD) algorithm in the OTB 9.0.0 plugin, which was integrated into QGIS version 3.24, to obtain the changes in the different LULC classes for the periods considered in this study. The MAD algorithm produces a set of N change maps, where N is the maximum number of bands in the first and second input images [68]. In addition, the results of the distribution of LULC areas were used to calculate occupancy and use trends, net changes, percentage changes and LULC rates between the years 1994, 2003, 2013 and 2022. The overall rate of change (Tg) is used to estimate the overall increase (the proportion of gain or loss) in the area of LULC units [58]. It is obtained from the following mathematical formula (7):

 doi:10.20944/preprints202412.0754.v1

$$TG = [\frac{S2 - S1}{S1}] \times 100 \quad (7)$$

where Tg is the overall rate of change (%); S1 represents the area of the class at date t_1 (initial date); and S2 is the area of the class at date t_2 (final date).

To obtain the annual rate of change for each type of LULC, the rate of change for the previous year was subtracted from that for the initial year and then divided by the total number of years [24]. This is obtained via equation (8).

$$TV = \frac{TF - TI}{N} \quad (8)$$

where TV is the rate of change; TF is the final year; TI is the initial year; and N is the number of years between two analysis dates.

A post classification change map was then produced to visualise these changes. The product of change detection via the MAD algorithm was overlaid with the LULC classes for each year to identify the nature of the change (change from class a to class b). This technique for detecting post classification changes provides important information about the conversions that have taken place between the different LULC classes.

2.2.6. Correlation Analysis Between the Variations in LULC Classes

The Pearson coefficient (r) was estimated to assess the linear correlation between the variation in built-up areas and that of the other LULC classes. This coefficient ranges from -1 to +1, where -1 indicates a perfect negative correlation, +1 indicates a perfect positive correlation and 0 indicates that there is no linear correlation between the variables [50,58]. Next, the coefficient of determination (R^2) was determined via simple linear regression to estimate the percentage of variance shared between the variation in built-up areas and that in the other LULC classes [69]. The simple linear regression model was run via R-studio software version 4.4.1. The Pearson correlation coefficient is expressed in equation (9):

$$rxy = \frac{n\sum xiyi - \sum xi \sum yi}{\sqrt{n\sum xi^2 - (\sum xi)^2}\sqrt{n\sum yi^2 - (\sum yi)^2}} \quad (9)$$

where rxy is the Pearson correlation coefficient r between x and y, n is the number of observations, x i is the value of x (for the ith observation) and y i is the value of y (for the nth observation).

2.2.7. Analysis of Built-Up Area Growth and the Population Growth Rate

The average annual of urban land consumption rate (ULCR) was calculated between the different analysis years. The average urban land consumption rate is an important indicator for understanding the rate of expansion of a city [10]. It is calculated via equation (10):

$$ULCR = \frac{LN\left(\frac{U_2}{U_1}\right)}{n} \times 10 \quad (10)$$

where U_2 = built-up area in the Sarh town at final year; U_1 = built-up area in the Sarh town at initial year; n is the number of the years between t_2 and t_1.

The average annual growth rate of the population (PGR) is an important indicator for understanding the rate of population growth for the period between two general censuses [70]. It is calculated via equation (11):

$$PGR = \frac{LN\left(\frac{P_2}{P_1}\right)}{n} \times 10 \quad (11)$$

where P_2 = population counted in Sarh town at final year; P_1= population counted in Sarh town at initial year; n is the number between two censuses.

The efficiency and sustainability of land use in Sarh town was assessed on the basis of indicator 11.3.1 of Sustainable Development Goals [71,72]. It is defined as the ratio between the average rate of urban land consumption and the average rate of population growth [73,74]. A ratio (ULCR/PGR) ≈ 1 indicates that urban land consumption was almost equivalent to the rate of population growth. A

 doi:10.20944/preprints202412.0754.v1

ratio (ULCR/PGR) < 1 indicates urban land consumption at a slower rate than its population has grown. On the other hand, a ratio (ULCR/PGR) > 1 indicates that urban land has been consumed faster than the population has grown. The ratio between ULCR and PGR was calculated using the following equation (12).

$$\text{ULCR/PGR} = \frac{\text{ULCR}}{\text{PGR}} \quad (12)$$

where ULCR/PGR is the ratio of ULCR to PGR, ULCR is the average rate of consumption of urban land (built-up areas in the town), and PGR is the average annual growth rate of the population.

2.2.8. Key Informant Interviews

To increase the robustness of the analysis of the dataset used for this study, qualitative data were collected via interviews with key informants. These were civil servants/employees from the technical services of the land registry, environment and urban planning of the provincial delegation of planning, housing development and urban planning of the Moyen-Chari province. The interview questions concerned the principles of land allocation in force in Sarh town, land management, the causes and factors of the degradation of green spaces, and the challenges associated with the occupation and use of urban land. These data were analysed to gain a better understanding of the correlation observed between the expansion of built-up areas and the loss of vegetation in Sarh town.

3. Results

3.1. Dynamics of Land Use and Land Cover (LULC)

Sarh town has undergone a significant change in LULC, marked by a sharp increase in built-up areas. An analysis of the results of the classification evaluation via the random forest algorithm reveals the accuracy at the pixel level, the values of which are shown in Table 2 below.

Table 2. Overall accuracy of Random Forest classification.

Years	Kappa index	Overall accuracy	Years
2022	93.31	94.33	2022
2013	91.66	93.10	2013
2003	87.00	91.33	2003
1994	86.65	90.25	1994

As the overall accuracy values are between 90.25% and 94.33%, we can confirm that the classification is good enough for an analysis of land use dynamics.

To validate the classification results obtained via the random forest, these results were compared with real-life observations provided by Google Earth pro ortho photos, cadastral maps and field data. These operations increased the accuracy of the results. Table 3 below summarises the areas of misclassified parcels that have been reclassified.

Table 3. Summary of areas of misclassified plots.

Area in hectares (ha) of reclassified plots				
LULC	**1994**	**2003**	**2013**	**2022**
Built-up area	35.28	30.78	20.67	25.66
Vegetation	16.65	15.06	12.74	09.23
Bare Land	51.28	45.66	40.86	33.13
Water area	2.16	0.01	0.0	0.0

Between 1994 and 2022, the growth of Sarh town resulted in a sharp increase in built-up areas to the detriment of vegetation and bare land (Table 4). The surface area of built-up areas has increased

 doi:10.20944/preprints202412.0754.v1

from 806.46 ha in 1994 to 2603.52 ha in 2022. Moreover, the area of vegetation has decreased considerably, from 758.65 ha to 231.18 ha. Similarly, bare land has decreased significantly, from 2095.57 ha to 922.37 ha. The change in water area is not significant. Over time, there was a considerable increase in built-up areas, whereas the areas of bare vegetation and land decreased (Figure 3).

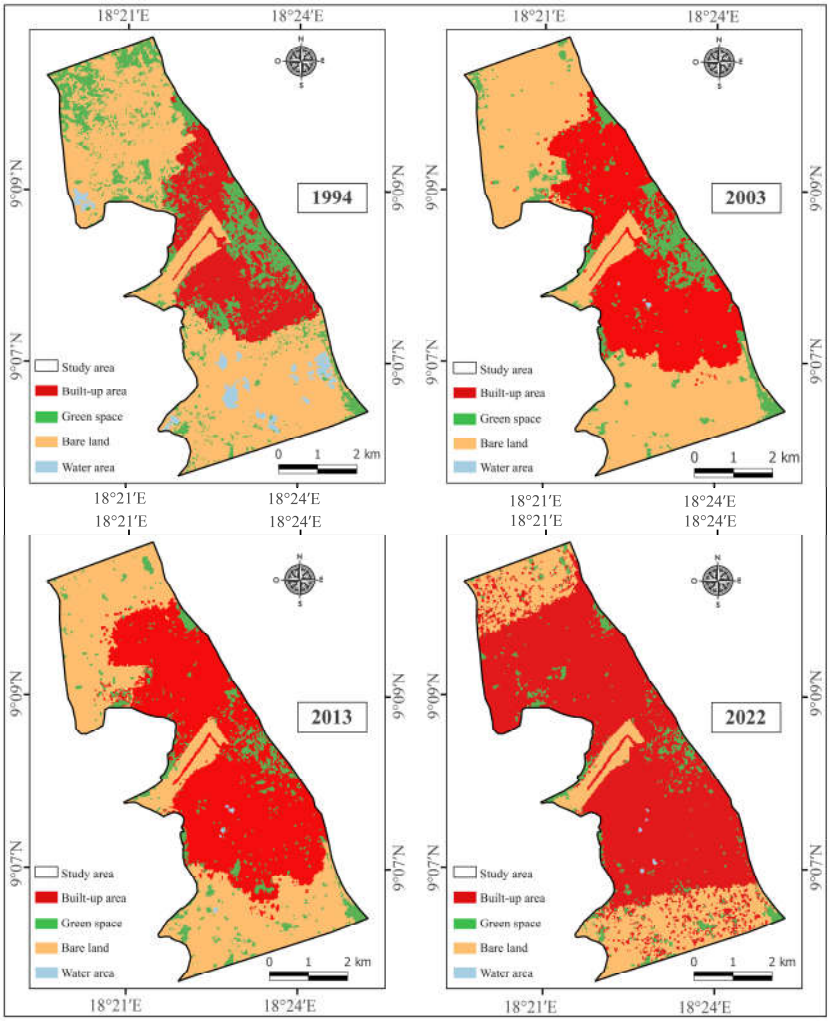

Figure 3. Sarh LULC from 1994 to 2022.

Table 4. Occupation and use of space in relation to LULC classes in Sarh town from 1994-2022.

Classes	Area in hectares and percentage by year of analysis							
	1994 (%)		2003 (%)		2013 (%)		2022 (%)	
Built-up area	806.46	21.44	1420.97	37.78	1815.78	48.28	2603.52	69.23
Vegetation	758.65	20.17	422.35	11.23	327.23	8.70	231.18	6.15
Bare land	2095.57	55.72	1915.10	50.92	1612.98	42.89	922.37	24.52
Water area	100.27	2.67	2.52	0.07	4.95	0.13	3.87	0.10
Total	3760.89	100.00	3760.89	100.00	3760.89	100.00	3760.89	100.00

3.1.1. Correlation Analysis Between Variation in Built-Up Areas and Other LULC Classes

Table 5 below shows significant correlations between built-up areas and vegetation and between built-up areas and bare land. There is a negative correlation ($r = -0.974$, $R^2 = 0.950$) between built-up areas and bare land. There was a strong negative correlation ($r = -0.930$, $R^2 = 0.86$) between built-up

Preprints.org (www.preprints.org) | NOT PEER-REVIEWED | Posted: 10 December 2024 doi:10.20944/preprints202412.0754.v1

areas and vegetation. On the other hand, the correlation between built-up areas and water areas (r= 0.751, R^2 = 0.562) is moderate and not significant.

Table 5. Correlation between built-up areas and other occupancy classes.

Correlation type	Coefficient of Correlation (r)	Determination coefficient (R^2)
Built-up area & vegetation	-0.930	0.864
Built-up area & water area	-0.751	0.562
Built-up area & bare land	-0.974	0.950

The strong negative correlation between built-up areas and vegetation, on the one hand, and between built-up areas and bare land, on the other hand, shows that the variation in vegetation and bare land in Sarh town is explained by the variation in built-up areas (Figure 4).

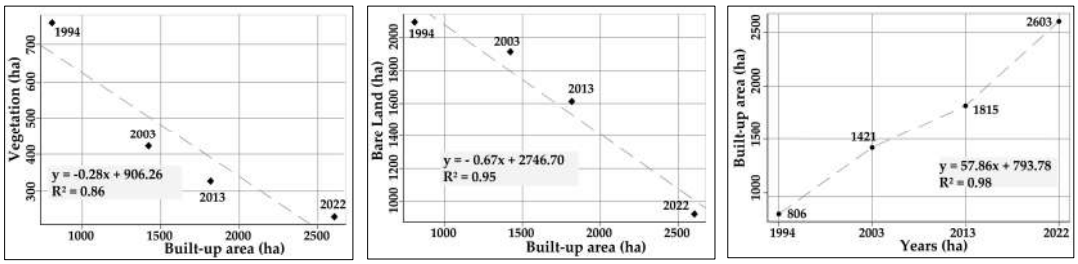

Figure 4. Linear regression models: **(a)** between built-up areas and vegetation; **(b)** between built-up areas and bare land; **(c)** between built-up areas and years of observation.

Somes direct observations during the fieldwork made it possible to identify certain green spaces used for construction (Figure 5).

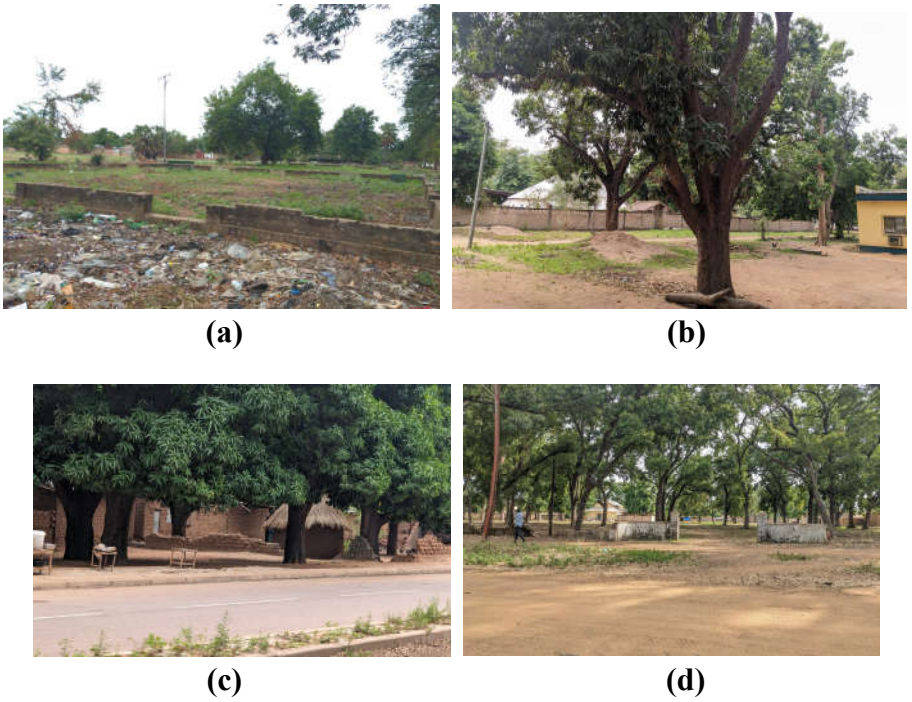

Figure 5. Photos illustrating the vegetations areas used for built-up areas: **(a)** and **(b)** in the residential district; **(c)** in the garden district; and **(d)** in the Blablim district.

 doi:10.20944/preprints202412.0754.v1

Between 1994 and 2022, the urban space varied according to the built-up areas (dense zone, moderate zone, and weak zone). Over time, the town has become progressively denser from the center outwards, particularly to the north and south (Figure 6). Expansion to the east and west is limited by the presence of the Chari and Bahr-Kôh Rivers. The surrounding village cores have gradually been integrated into the town. For example, Kemkian, Maïlaou, Badi, Kissimi and Maïgara 2, which were once small villages, gradually became neighbourhoods of Sarh.

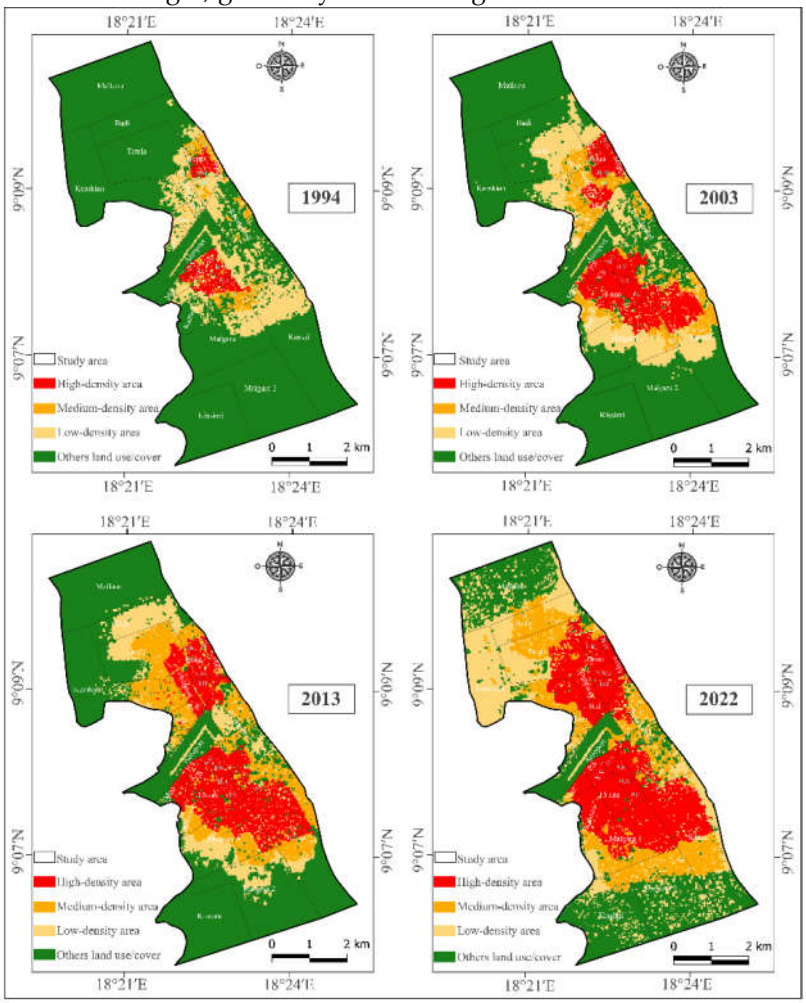

Figure 6. Dynamics of built-up areas in Sarh town from 1994 to 2022.

Table 6 below shows the change in surface areas in hectares and percentages of built-up areas between 1994 and 2022. There has been a sharp increase in densely built-up areas, from 127.71 ha in 1994 to 1034.86 ha in 2022. Similarly, medium and low-density built-up areas increased from 102.19 ha to 666.47 ha and from 576.37 ha to 902.32 ha, respectively.

Table 6. Land use and land cover zones centred on built-up areas.

Classes	**Area in hectares and percentage by year of analysis**							
Years	**1994 (%)**		**2003 (%)**		**2013 (%)**		**2022 (%)**	
High built-up area	127.71	3.30	454.26	11.99	683.89	18.18	1034.86	27.51
Medium built-up area	102.19	2.72	265.85	7.08	574.41	15.27	666.47	17.73
Low built-up area	576.37	15.34	701.27	18.66	557.57	14.82	902.32	23.99
Others	2954.63	78.64	2339.97	62.27	1945.02	51.73	1157.24	30.77
Total	3760.89	100.00	3760.89	100.00	3760.89	100.00	3760.89	100.00

 doi:10.20944/preprints202412.0754.v1

From 1994 to 2022, there was a significant conversion of other land occupation and the use of classes to built-up areas. This transformation results from the occupation of bare land and green spaces in favour of built-up areas. For example, some green spaces in the residential, Kemkian, Maïlaou, Badi, Kissimi and Maïgara 2 neighbourhoods have gradually been used for construction (dense, medium, low-density). In addition, low-density areas have been converted to high-density areas, as in the Kassaï, Kamati, Maroc, Maigara 1, Tombalbaye and Gardolet districts, which were previously low-density peripheral areas. On the other hand, the conversion of moderately dense areas and high-density areas to other land-use classes is negligible. Figure 7 below illustrates the conversions of the different land use and land cover classes from 1994 to 2022.

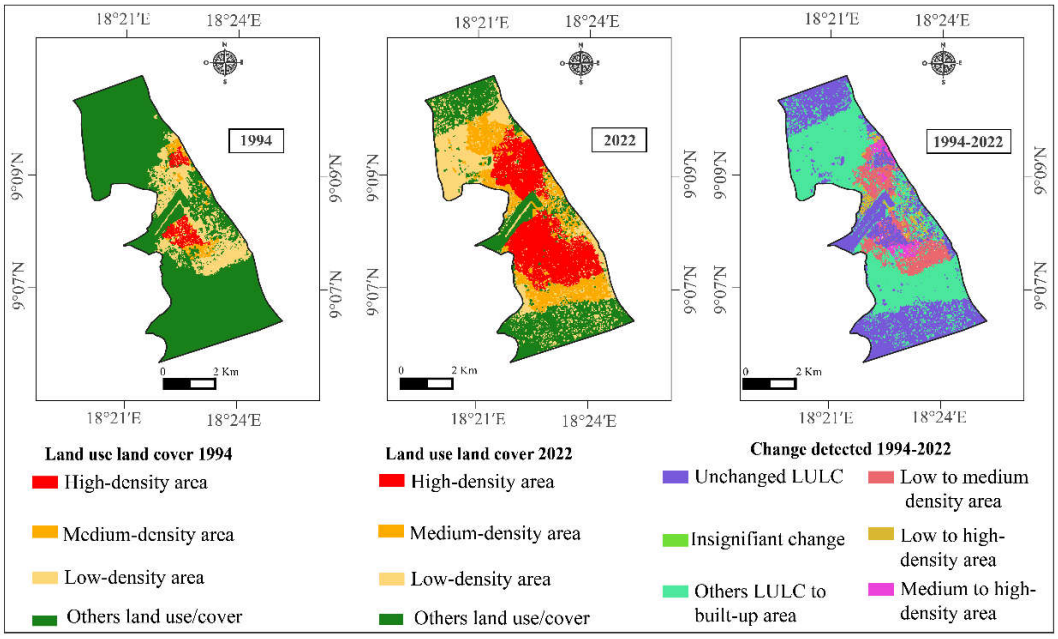

Figure 7. Changes in land use and tenure between 1994 and 2022.

Some direct observations during the fieldwork enabled us to identify certain buildings in small villages integrated into the town that always retained their village character (Figure 8).

(a) **(b)**

Figure 8. (a) Photo of the buildings in the Kissimi village core integrated into the town. **(b)** Photo of new buildings on the northern outskirts of the town.

3.1.2. Trends and Variation Matrix for Land Use in Sarh Town

The study revealed an increase in built-up areas (dense, medium-density and low-density areas). Between 1994 and 2022, the rates of change increased. The highest rates of change are observed in the high-density built-up area (24.40 ha/year) and the medium-density built-up area (19.03 ha/year). There was also an upwards trend in the low-density built-up area (1.94 ha/year), except for the period from 2003-2013, when there was a decline (-0.70 ha/year).

 doi:10.20944/preprints202412.0754.v1

The unbuilt areas, vegetation, and water areas experienced decreases in area between 1994 and 2022, indicating a decrease in the rate of change. The maximum rate of change (-2.09 ha) was observed over the period from 1994--2022 for vegetated and unbuilt areas. **Figure 9** below illustrates the changes in built-up areas (dense, medium-density and low-density areas) and other occupancy classes (vegetation, unbuilt areas and water areas).

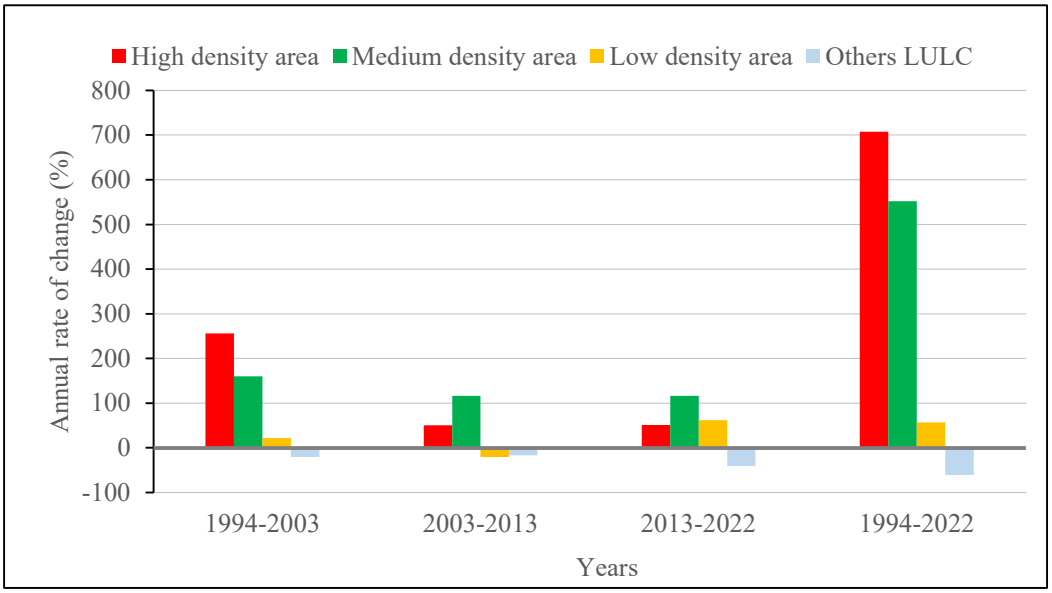

Figure 9. Trends in changes in occupation and use between periods.

The land use and land cover change (LULC) matrix for Sarh town between 1994 and 2022 revealed the conversion of various LULC classes into other classes **(Table 7**). The increase in the area of high-density built-up areas during this period was due mainly to the conversion of vegetation, undeveloped areas and low-density built-up areas. Low-density built-up areas are the main LULC classes that have been converted to high-density built-up areas, except for the period 2013-2022, when a significant increase in medium-density built-up areas was observed. The decrease in the other LULC classes (vegetation, unbuilt area) is the result of their conversion to built-up areas (dense, medium-density and low-density).

Table 7. Occupancy and use of a class change matrix (LULC).

Années	LULC	High built-up area	Medium built-up area	Low built-up area	Others LULC	Total
1994-2003	**High built-up area**	127.71	0.63	3.06	0.81	127.71
	Medium built-up	74.85	12.47	10.90	3.95	102.19
	Low built-up area	209.34	146.34	179.71	40.97	576.37
	Others LULC	46.85	106.40	507.60	2293.78	2954.62
	Total (ha)	454.26	265.85	701.27	2239.51	3760.89
2003-2013	**High built-up area**	405.86	13.14	31.33	2.79	409.25
	Medium built-up	118.66	115.10	24.63	7.62	691.15
	Low built-up area	133.62	369.37	163.45	35.46	320.49
	Others LULC	25.76	76.80	338.15	1899.37	2340.00
	Total (ha)	683.89	574.41	557.57	1945.26	3760.89
2013-2022	**High built-up area**	648.86	12.39	19.69	2.95	683.89
	Medium built-up	227.36	235.86	104.41	6.78	574.41

 doi:10.20944/preprints202412.0754.v1

	Low built-up area	132.14	260.31	131.91	33.20	557.57
	Others LULC	26.50	157.90	646.30	1114.31	1945.02
	Total (ha)	1034.86	666.47	902.32	1157.24	3760.89
	High built-up area	123.60	3.75	0.27	0.09	127.71
	Medium built-up	87.15	11.17	3.33	0.54	102.19
1994-2022	**Low built-up area**	409.35	77.58	76.07	13.37	576.37
	Others LULC	411.37	577.63	822.25	1143.38	2954.63
	Total (ha)	1034.86	666.38	901.92	1157.38	3760.89

3.2. Analysis of Growth in Built-Up Areas in Relation to Population Growth

The results in Figure 10 below show a dynamic change between the urban land consumption rate (ULCR) and the population growth rate (PGR) between 1994 and 2022. Initially, from 1994 to 2003, the ULCR far exceeded the PGR, indicating rapid urbanisation. However, from 2003 to 2013, the PGR began to exceed the ULCR, resulting in increased pressure on urban resources. Between 2013 and 2022, although both indicators increased, the ratio remained below 1, indicating that population growth remained higher than the expansion of built-up areas. Over the study period from 1994 to 2022, the results show a ratio of 1.255. This indicates that land use was more dynamic than population growth was during this period.

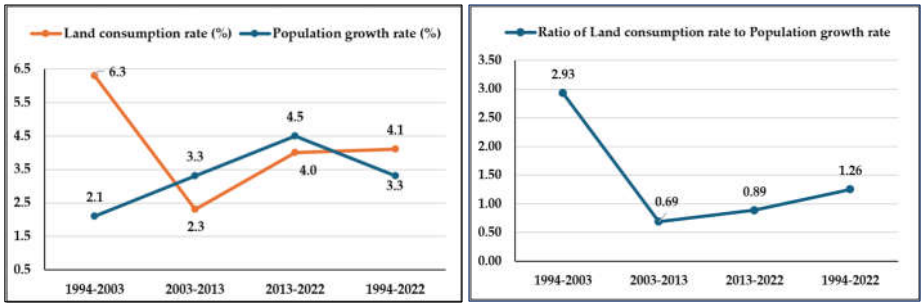

(a) **(b)**

Figure 10. a) Land consumption rate (%) and Population growth rate (%). b) Ratio of Land consumption to population growth rate.

3.3. Development Challenges and Sustainable Land Use in Sarh

The various interviews with key informants revealed that the spatial expansion of Sarh town was the result of several factors. First, population growth and the growing demand for housing, which requires access to land, have not been effectively managed by authorities, particularly in a context where property policies are still at an early stage of development. This has led to the proliferation of spontaneous occupation, exacerbating land speculation. Owing to their inadequate skills and limited means of intervention, public players find it difficult to apply regulations on land and urban management.

In addition to these observations, there is no budget line dedicated to the maintenance and restoration of green spaces. In the past, as part of the National Tree Week initiated by President Ngarta Tombalbaye in September 1972, a budget of between five hundred thousand and one million CFA francs was allocated to these activities. However, this budget has not been allocated to local authorities for over twenty years. In addition, there is a lack of public awareness of the importance of these areas, exacerbated by financial constraints. In addition, the lack of human resources within the department responsible for the environment, as well as the lack of collaboration between municipal services and those responsible for land management, are all factors contributing to the deterioration of vegetation in Sarh town.

 doi:10.20944/preprints202412.0754.v1

4. Discussion

The classification results obtained via the random forest (RF) algorithm revealed overall accuracies and kappa indices ranging from 86% to 95%, demonstrating an overall satisfactory classification. This algorithm was chosen for its recognised performance in predicting land cover, particularly in topographically complex areas. RF is currently considered one of the best performing algorithms for land cover classification in topographically complex areas via remote sensing data [62]. According to Aka et al. [58], classification via remote sensing data is considered acceptable when the value of the kappa coefficient exceeds 75%. An accuracy of more than 85% is generally considered adequate for effective classification [12]. These results unequivocally indicate the statistical validity of our analysis. However, it is important to note that the mapping of heterogeneous spaces, such as urban areas, using Landsat satellite images with a spatial resolution of 30 × 30 m has limitations, particularly with respect to distinguishing between built-up areas and unbuilt areas. This difficulty has an impact on the accuracy of classification. Although PCAs were performed using indices derived from primary channels to maximise band information and eliminate noise [24], they failed to provide sufficient distinguishing data to differentiate built-up areas from bare land. The kappa index alone is not sufficient to assess the accuracy of a classification fully [19]. This limitation highlights the need for cross-validation with field data to fill potential gaps in the classification. The validation approach using complementary data adopted in this study contributed to improving the accuracy of the results. This finding is in line with other research results, which have also revealed a significant improvement in classification accuracy owing to the integration of field data [67].

The results of the land use and occupancy dynamics (LULC) analysis revealed a rapid expansion of built-up areas in Sarh town. These results are consistent with those of previous studies conducted in small urban centers such as Calabar in Nigeria [30], Bou Saâda in Algeria [32], Solwezi in Zambia [31], Ma'an in Jordan [74] and Kwabre East in Ghana [33]. In Sarh, the expansion of built-up areas has been to the detriment of vegetated areas and bare land. Simple linear regression analysis revealed a strong negative correlation between the increase in built-up land and the loss of vegetation, indicating that the latter was due mainly to the expansion of built-up areas. This result corroborates that of Akpu et al. [25], who reported a similar negative correlation in their study area, where 68% of the vegetation loss was attributable to urban expansion. The observed reduction in vegetation cover is consistent with the findings of similar studies, which highlighted a significant loss of vegetated area due to the expansion of built-up areas [42,68,69]. Munyati and Drummond [75] reported losses in both the quantity and quality of green spaces in Mafikeng, South Africa, due to the conversion of these spaces for the construction of social amenities such as schools and housing. The rapid expansion of built-up areas at the expense of vegetation is a challenge for environmental sustainability, particularly in developing countries [76]. Dieng and Keita [77] noted that the uncontrolled urbanisation of cities contributes significantly to the vulnerability of the urban environment. Furthermore, the loss of bare land to the detriment of built-up areas corroborates the findings of rapid urban expansion to the detriment of bare land in different study areas [8,73].

This study revealed a variation in built-up areas (dense, medium-density and low-density) in Sarh town. The densification of the town has progressively moved from the center to the periphery, particularly to the north and south. These changes include the gradual integration of small villages into towns and the transformation of low- and medium-density areas into dense areas. Similar results were observed in the study of the dynamics of built-up areas in the Grand Lomé district of Togo via Landsat imagery [24]. This evolution is characterised by high rates of change for high-density and medium-density built-up areas. On the other hand, low-density areas also exhibited growth, with the exception of the period 2003-2013, during which a regression was observed. These changes manifest themselves in time and space, notably through the expansion of built-up areas and the intensification of land-use changes, leading to modifications and alterations. These results confirm the hypothesis that anthropogenic activities influence the land surface, leading to an increase in urban sprawl [79]. Chmielewski et al. [80] reported that in some regions, anthropogenic impacts occur on an unprecedented scale, qualifying as ecocatastrophes whose effects extend beyond local boundaries.

 doi:10.20944/preprints202412.0754.v1

From 1994 to 2022, urban land use was more dynamic than population growth was, illustrating an urban sprawl phenomenon marked by the appearance of new buildings on the outskirts of Sarh town. This finding corroborates the findings of Mohamed et al. [81], who confirmed that the effects of the sprawl pattern strongly influence the dynamics of the built-up area of the Oromia region more than population growth does. The sprawl of Sarh town is the result of a preference for single-family homes and more spacious housing, as well as the conversion of rural areas into urban zones. This rapid expansion is likely to exacerbate socio-spatial disparities. For example, there is an imbalance in the distribution of basic infrastructure and facilities between the outlying districts (north and south) and the central districts. A compact city will be more functional because activities and services will be closer to the population, making travel and the provision of urban infrastructure less costly [52]. According to Wellmann et al. [23], compact and dispersed cities are considered sustainable urban forms. Moreover, urban sprawl contributes to fragmentation and impoverishment [35]. One of the major consequences of uncontrolled urbanisation in Sarh town is flooding, of which the 2024 flood was the most catastrophic. Although flooding is caused by many factors, such as pollution and climatic conditions, urbanisation plays an important role by leading to poor rainfall management and a lack of water drainage due to construction [35]. Urban expansion could also lead to an increase in surface runoff and changes in drainage geography, leading to urban flooding [8].

5. Conclusion

The aim of this study is to inform the scientific community about the degree of expansion of built-up areas and the loss of vegetation in Sarh town in southern Chad. First, diachronic analysis of satellite images via remote sensing and geographic information system tools revealed that the expansion of Sarh town has resulted in an increase in built-up areas to the detriment of vegetation and bare land. The results also revealed a strong negative correlation between the growth of built-up areas and the loss of vegetation. In addition, growth in built-up areas has been more dynamic than population growth over the study period (1994-2022). Field surveys reveal that this situation is due to a preference for more spacious housing, inadequate land management and limited resources for the rehabilitation of vegetation. These results follow critical debates on sustainable land management in the context of the rapid expansion of secondary towns in Africa. However, the limited spatial resolution of Landsat, the influence of cloud cover and the availability of images during all periods of the year meant that it was not possible to obtain more complete and accurate results. In addition, owing to the unavailability of demographic data for each period, the analysis was sometimes based on demographic projections. Consequently, further in-depth studies using other data sources are needed to obtain more complete and accurate results.

To achieve sustainable urban development, it is essential to have a precise understanding of how land is occupied and used. Local authorities will therefore need effective tools to enable them to update spatial data on an ongoing basis, thereby facilitating better management of the rapid expansion of urban areas. In addition, the use of spatial remote sensing and geographic information system (GIS) tools is necessary to enable town managers to monitor urban growth and the accompanying spatial transformations.

Author Contributions: Conceptualization, F.T.N. and M.L.S.; methodology, F.T.N., J.K.S.A., M.L.S. and A.B.M.; software, F.T.N., J.K.S.A. and A.B.M.; validation, J.K.S.A., A.B.M.; investigation and formal analysis, F.T.N., B.P.S. and A.P.T.; data curation, F.T.N., B.P.S. and A.P.T.; writing- original draft preparation, F.T.N. and M.L.S.; writing-review and editing, F.T.N. and M.L.S.; resources, F.T.N., N.T. and F.H.; supervision, N.T. and F.H.; project administration, N.T. and F.H.; visualisation, N.T. and F.H.; funding acquisition, F.T.N. All authors have read and agreed to the published version of the manuscript.

Funding: This research is funded by the World Bank. The funding number is 6512-TG & 5360-TG.

Data availability statement: Data is contained within the article or supplementary material.

Acknowledgments: The authors would like to thank the Regional Center of Excellence on Sustainable Cities in Africa (CERViDA-DOUNEDON), the Association of African Universities and the World Bank Group for their financial support.

Conflicts of interest: The authors declare no conflicts of interest.

References

1. Wubie, A. M.; De Vries, W. T.; Alemie, B. K. A Socio-Spatial Analysis of Land Use Dynamics and Process of Land Intervention in the Peri-Urban Areas of Bahir Dar City. *Land* **2020**, 9, 445. doi: 10.3390/land9110445
2. Liu, J.; Heiskanen, J.; Aynekulu, E.; Pellikka, P. K. E. Seasonal variation of land cover classification accuracy of Landsat 8 images in Burkina Faso. *Int. Arch. Photogramm. Remote Sens. Spat. Inf. Sci.* **2015**, XL-7/W3, 455-460. doi: 10.5194/isprsarchives-XL-7-W3-455-2015
3. Nkeki, F. N. Spatio-temporal analysis of land use transition and urban growth characterization in Benin metropolitan region, Nigeria. *Remote Sens. Appl. Soc. Environ.* **2016**, 4, 19-137. doi: 10.1016/j.rsase.2016.08.002
4. Zhou, Y.; Li, X.; Asrar, G. R.; Smith, S. J.; Imhoff, M. A global record of annual urban dynamics (1992–2013) from nighttime lights », *Remote Sens. Environ.* **2018**, 219, 206-220. doi: 10.1016/j.rse.2018.10.015
5. Nor, A. N. M.; Corstanje, R.; Harris, J. A.; Brewer, T. Impact of rapid urban expansion on green space structure. *Ecological Indicators* **2017**, 81, 274-284. https://doi.org/10.1016/j.ecolind.2017.05.031
6. Vasenev, V. I.; Stoorvogel, J. J.; Leemans, R.; Valentini, R.; Hajiaghayeva, R. A. Projection of urban expansion and related changes in soil carbon stocks in the Moscow Region. *J. Clean. Prod.* **2017,** 170, 902-914. doi: 10.1016/j.jclepro.2017.09.161
7. Chen, J.; Yu, Z.; Li, M.; Huang, X. Assessing the Spatiotemporal Dynamics of Vegetation Coverage in Urban Built-Up Areas. *Land* **2023**, 12, 235. doi: 10.3390/land12010235
8. Ibrahim Mahmoud, M.; Duker, A.; Conrad, C.; Thiel, M.; Shaba Ahmad, H. Analysis of Settlement Expansion and Urban Growth Modelling Using Geoinformation for Assessing Potential Impacts of Urbanization on Climate in Abuja City, Nigeria. *Remote Sens.* **2016**, 8, 220. doi: 10.3390/rs8030220
9. Forget, Y.; Shimoni, M.; Gilbert, M.; Linard, C. Mapping 20 Years of Urban Expansion in 45 Urban Areas of Sub-Saharan Africa. *Remote Sens.* **2021**, 13, 525. doi: 10.3390/rs13030525
10. Kukkonen, M. O.; Muhammad, M. J.; Käyhkö, N.; Luoto, M. Urban expansion in Zanzibar City, Tanzania: Analyzing quantity, spatial patterns and effects of alternative planning approaches. *Land Use Policy* **2018**, 71, 554-565. doi: 10.1016/j.landusepol.2017.11.007
11. Moisa, M. B.; Gemeda, D. O. Analysis of urban expansion and land use/land cover changes using geospatial techniques: a case of Addis Ababa City, Ethiopia. *Appl. Geomat.* **2021**, 13, p. 853-861. doi: 10.1007/s12518-021-00397-w
12. Das, M.; Das, A. Dynamics of Urbanization and its impact on Urban Ecosystem Services (UESs): A study of a medium size town of West Bengal, Eastern India. *J. Urban Manag.* **2019**, 8, 420-434. doi: 10.1016/j.jum.2019.03.002
13. Teadoum Naringué, F.; Tob-Ro, N.; Allarané, N.; Azagoun, V. V. A.; Hetcheli, F. Factors hindering the implementation of urban planning tools in Central Africa: Case study of reference urban plan for Sarh Town (Chad). *J. Infrastruct. Policy Dev.* **2024**, 8, 8409. doi: 10.24294/jipd8409
14. Cities Alliance. The Role of Secondary Cities in a National System of Cities. Available online: https://www.citiesalliance.org/themes/secondary-cities?page=0 (Accessed on 15 October 2024).
15. Tripathi, S.; Mitra, A. Shedding light on unnoticed gems in India: A small town's growth perspective. *Land Use Policy* **2022**, 120, 106239. doi: 10.1016/j.landusepol.2022.106239
16. Maru, M.; Worku, H.; Birkmann, J. Factors affecting the spatial resilience of Ethiopia's secondary cities to urban uncertainties: A study of household perceptions of Kombolcha city. *Heliyon* **2021**, 7, e08472. doi: 10.1016/j.heliyon.2021.e08472

17. Schug, F.; Okujeni, A.; Hauer, J.; Hostert, P.; Nielsen, J. Ø.; Van Der Linden, S. Mapping patterns of urban development in Ouagadougou, Burkina Faso, using machine learning regression modeling with bi-seasonal Landsat time series. *Remote Sens. Environ.* **2018**, 210, 217-228. doi: 10.1016/j.rse.2018.03.022
18. Akintunde, J. A.; Adzandeh, E. A.; Fabiyi, O. O. Spatio-temporal pattern of urban growth in Jos Metropolis, Nigeria. *Remote Sens. Appl. Soc. Environ.* **2016**, 4, 44-54. doi: 10.1016/j.rsase.2016.04.003
19. Dan-Jumbo, N. G.; Metzger, M. J.; Clark, A. P. Urban Land-Use Dynamics in the Niger Delta: The Case of Greater Port Harcourt Watershed. *Urban Sci.* **2018**, 2, 108. doi: 10.3390/urbansci2040108
20. Elagouz, M. H.; Abou-Shleel, S. M.; Belal, A. A.; El-Mohandes, M. A. O. Detection of land use/cover change in Egyptian Nile Delta using remote sensing. *Egypt. J. Remote Sens. Space Sci.* **2020**, 23, 57-62. doi: 10.1016/j.ejrs.2018.10.004
21. Hou, H.; Estoque, R. C.; Murayama, Y. Spatiotemporal analysis of urban growth in three African capital cities: A grid-cell-based analysis using remote sensing data », *J. Afr. Earth Sci.* **2016**, 123, 381-391. doi: 10.1016/j.jafrearsci.2016.08.014
22. Serasinghe Pathiranage, I. S.; Kantakumar L. N.; Sundaramoorthy, S. Remote Sensing Data and SLEUTH Urban Growth Model: As Decision Support Tools for Urban Planning. *Chin. Geogr. Sci.* **2018**, 28, 274-286. doi: 10.1007/s11769-018-0946-6
23. Wellmann, T.; Schug, F.; Haase, D; Pflugmacher, D.; S. Van Der Linden. Green growth? On the relation between population density, land use and vegetation cover fractions in a city using a 30-years Landsat time series. *Landsc. Urban Plan.* **2020**, 202,103857. doi: 10.1016/j.landurbplan.2020.103857
24. Blakime, T.-H.; Adjonou, K.; Komi, K.; Hlovor, A. K. D.; Gbafa, K. S.; Zoungrana; J.-B. B., Polorigni; B.; Kokou, K. Dynamics of Built-Up Areas and Challenges of Planning and Development of Urban Zone of Greater Lomé in Togo, West Africa. *Land* **2024**, 13, 84. https://doi.org/10.3390/land13010084
25. Akpu, B.; Tanko, A.; Jeb, D.; Dogo, B. Geospatial Analysis of Urban Expansion and Its Impact on Vegetation Cover in Kaduna Metropolis, Nigeria. *Asian J. Environ. Ecol.* **2017**, 3, 1-11. doi: 10.9734/AJEE/2017/31149
26. Abo-El-Wafa, H.; Yeshitela, K.; Pauleit, S. The use of urban spatial scenario design model as a strategic planning tool for Addis Ababa », *Landsc. Urban Plan.* **2018,** 180, 308-318. doi: 10.1016/j.landurbplan.2017.08.004
27. Nshimiyimana, A. R.; Niyigena, E.; Nyandwi, E.; Ngwijabagabo, H.; Rugengamanzi, G. Spatial Assessment of Urban Growth on Green Spaces in Rwanda: An insight from Rebero Mountain Landscape in Kicukiro District, City of Kigali. *Rwanda J. Eng. Sci. Technol. Environ.* **2023,** 5, 1. doi: 10.4314/rjeste.v5i1.5
28. Seth, A.-O.; Kwaku, K. M.; Michael, O. A; Owusu, A. Tragedy of urban green spaces depletion in selected sub-Sahara African major cities. *J. Afr. Stud. Dev.* **2023**, 15, 46-61. doi: 10.5897/JASD2023.0682
29. Ammann, C.; Sanogo, A.; Heer, B. Secondary Cities in West Africa: Urbanity, Power, and Aspirations. *Urban Forum* **2022**, 33, 445-461. doi: 10.1007/s12132-021-09449-1
30. Awuh, M. E.; Officha, M. C.; Okolie, A. O.; Enete, I. C. Land-Use/Land-Cover Dynamics in Calabar Metropolis Using a Combined Approach of Remote Sensing and GIS. *J. Geogr. Inf. Syst.* **2018**, 10, 398-414. doi: 10.4236/jgis.2018.104021
31. Takam Tiamgne, X.; Kalaba, F. K.; Nyirenda, V. R. Land use and cover change dynamics in Zambia's Solwezi copper mining district. *Sci. Afr.* **2021**, 14, e01007. doi: 10.1016/j.sciaf.2021.e01007
32. Dechaicha, A.; Alkama, D. Suivi et quantification de l'urbanisation incontrôlée: une approche basée sur l'analyse multitemporelle des images satellitaires LANDSAT. Cas de la ville de Bou-Saada (Algérie). *Rev. Fr. Photogrammétrie Télédétection* **2021,** 223, 159-172. doi: 10.52638/rfpt.2021.595

33. Takyi, E.; Mensah, H.; Aazore, F. K.; Nalumu, D. J.; Abu, J. J. Understanding the Urban Planning-Green Space Depletion Nexus: Insights from the Kwabre East Municipality, Ghana. *Urban Forum* **2023**, 34, 19-342. doi: 10.1007/s12132-022-09471-x
34. Mahamat Hemchi, H.; Hallou, A. M. ; Danvidé, T. B. Analyse du processus d'extension de la ville de N'Djamena au Tchad (1900 – 2018). *Geo-Eco-Trop* **2021**, 45, 507-516. https://www.geoecotrop.be/uploads/publications/pub_453_10.pdf
35. EcoBioMania. 9 dangers de l'urbanisation non contrôlée sur l'environnement. Available online: https://www.ecobiomania.com/fr/dangers-urbanisation-non-contr%C3%B4l%C3%A9e-sur-environnement/ (Accessed on 01 November 2024).
36. Hamit, A.; Abdallah, M. N.; Abderamane, M.; Brahim, T.-I. A.; Bakay, B. D.; Aingar, B.; Oumar, D. T.; Julius, L. L. Assessment of the Vulnerability of the Shallow Aquifer of the City of Sarh in Chad, using the Drastic Approach. *Current Journal of Applied Science and Technology* **2021**, 1-10. https://doi.org/10.9734/cjast/2021/v40i1731428
37. INSEED. Principaux indicateurs globaux issus de l'analyse thématique du RGPH2. République du Tchad. 2012. Available online: https://unstats.un.org/unsd/demographic/sources/census/wphc/Chad/Chad_Resultats%20Globaux.pdf.(accessed on 05 September 2024).
38. Mairie de Sarh. Plan de Développement Communal de la commune de Sarh. Rapport définitif, République du Tchad, Sarh, 2018.
39. Amini, S.; Saber, M.; Rabiei-Dastjerdi, H.; Homayouni, S. Urban Land Use and Land Cover Change Analysis Using Random Forest Classification of Landsat Time Series. *Remote Sens.* **2022**, 14, 2654. doi: 10.3390/rs14112654
40. Bhatti, S. S.; Tripathi, N. K. Built-up area extraction using Landsat 8 OLI imagery. *GIScience Remote Sens.* **2014**, 51, 445-467. doi: 10.1080/15481603.2014.939539
41. Hashim, B. M.; Al Maliki, A.; Sultan, M. A.; Shahid, S.; Yaseen, Z. M. Effect of land use land cover changes on land surface temperature during 1984–2020: a case study of Baghdad city using landsat image. *Nat. Hazards* **2022**, 112, 1223-1246. doi: 10.1007/s11069-022-05224-y
42. Hu, Y.; Raza, A.; Syed, N. R.; Acharki, S.; Ray, R. L.; Hussain, S.; Dehghanisanij, H.; Zubair, M.; Elbeltagi, A. Land Use/Land Cover Change Detection and NDVI Estimation in Pakistan's Southern Punjab Province. *Sustainability* **2023**, *15*, 3572. https://doi.org/10.3390/su15043572
43. Mosammam, H. M.; Nia, J. T.; Khani, H.; Teymouri, A.; Kazemi, M. Monitoring land use change and measuring urban sprawl based on its spatial forms. *Egypt. J. Remote Sens. Space Sci.* **2017**, 20, 103-116. doi: 10.1016/j.ejrs.2016.08.002
44. Tew, Y. L.; Tan, M. L.; Samat, N.; Yang, X. Urban Expansion Analysis using Landsat Images in Penang, Malaysia. *Sains Malays.* **2019**, 48, 2307-2315. doi: 10.17576/jsm-2019-4811-02
45. Whitcraft, A. K.; Vermote, E. F.; Becker-Reshef, I.; Justice, C. O. Cloud cover throughout the agricultural growing season : Impacts on passive optical earth observations. *Remote Sensing of Environment* **2015**, *156*, 438-447. https://doi.org/10.1016/j.rse.2014.10.009
46. Bayode, T.; Siegmund, A. Tripartite relationship of urban planning, city growth, and health for sustainable development in Akure, Nigeria. *Front. Sustain. Cities* **2024**, 5, 1301397. doi: 10.3389/frsc.2023.1301397

47. Taiwo, B. E.; Kafy, A.-A.; Samuel, A. A.; Rahaman, Z. A.; Ayowole, O. E.; Shahrier, M.; Duti, B. M.; Rahman, M. T.; Peter, O. T.; Abosede, O. O. Monitoring and predicting the influences of land use/land cover change on cropland characteristics and drought severity using remote sensing techniques. *Environmental and Sustainability Indicators* **2023**, *18*, 100248. https://doi.org/10.1016/j.indic.2023.100248
48. U.S. Geological Survey. Landsat Collection 2 Level 2 Science Products: Fiche d'information US Geological Survey 2021–3055 (Fact Sheet), 2021. Available online: https://doi.org/10.3133/fs20213055 (Accessed on 14 September 2024)
49. Rahman, M.; Ullah, R.; Lan, M.; Sri Sumantyo J. T.; Kuze, H.; Tateishi, R. Comparison of Landsat image classification methods for detecting mangrove forests in Sundarbans. *Int. J. Remote Sens.* **2013**, 34, 1041-1056. doi: 10.1080/01431161.2012.717181
50. Fontana, A. G.; Nascimento, V. F.; Ometto, J. P.; Do Amaral, F. H. F. Analysis of past and future urban growth on a regional scale using remote sensing and machine learning. *Front. Remote Sens.* **2023**, 4, 1123254. doi: 10.3389/frsen.2023.1123254
51. Zhao, N.; Ma, A.; Zhong, Y.; Zhao, J.; Cao, L. Self-Training Classification Framework with Spatial-Contextual Information for Local Climate Zones. *Remote Sens.* **2019**, 11, 2828. doi: 10.3390/rs11232828
52. AZMI, R. Détection des changements dans les zones urbaines de la ville de Marrakech au Maroc par le biais du Google Earth Engine, Cours en ligne ouvert et massif, 2024. Available online: https://apps.courses.africancitieslab.org/learning/course/course-v1:UM6P+003+2022/block-v1:UM6P+003+2022+type@sequential+block@ad283ba090614980a65455eb26306c25/block-v1:UM6P+003+2022+type@vertical+block@c55d3d8e5c3c469aa715a93c91500aef (accessed on 14 June 2024).
53. Ettehadi Osgouei, P.; Kaya, S.; Sertel, E.; Alganci, U. Separating Built-Up Areas from Bare Land in Mediterranean Cities Using Sentinel-2A Imagery. *Remote Sens.* **2019**, 11, 345. doi: 10.3390/rs11030345
54. Fernández-Maldonado, V.; Navas, A. L.; Fabani, M. P.; Mazza, G.; Rodríguez, R. A Multi-Temporal Analysis on the Dynamics of the Impact of Land Use and Land Cover on NO2 and CO Emissions in Argentina for Sustainable Environmental Management. *Sustainability* **2024**, 16, 4400. doi: 10.3390/su16114400
55. Xu, H. Modification of normalised difference water index (NDWI) to enhance open water features in remotely sensed imagery. *Int. J. Remote Sens.* **2006**, 27, 3025-3033. doi: 10.1080/01431160600589179
56. Huete, A. R. A soil-adjusted vegetation index (SAVI). *Remote Sens. Environ.* **1988**, 25, 295-309. doi: 10.1016/0034-4257(88)90106-X
57. Breiman, L. Random Forests. *Mach. Learn.* **2001**, 45, 5-32. doi: 10.1023/A:1010933404324
58. Aka, K. S. R.; Akpavi, S.; Dibi, N. H.; Kabo-Bah, A. T.; Gyilbag, A.; Boamah, E. Toward understanding land use land cover changes and their effects on land surface temperature in yam production area, Côte d'Ivoire, Gontougo Region, using remote sensing and machine learning tools (Google Earth Engine). *Front. Remote Sens.* **2023**, 4, 1221757. doi: 10.3389/frsen.2023.1221757
59. Biau, G.; Scornet, E. A random forest guided tour. *TEST* **2016,** 25, 197-227. doi: 10.1007/s11749-016-0481-7
60. Gislason, P. O.; Benediktsson, J. A.; Sveinsson, J. R. Random Forests for land cover classification. *Pattern Recognit. Lett.* **2006**, 27, 294-300. doi: 10.1016/j.patrec.2005.08.011
61. Teluguntla, P.; Thenkabail, P. S.; Oliphant, A.; Xiong, J.; Gumma, M. K.; Congalton, R. G.; Yadav, K.; Huete, A. A 30-m landsat-derived cropland extent product of Australia and China using random forest machine learning algorithm on Google Earth Engine cloud computing platform. *ISPRS Journal of Photogrammetry and Remote Sensing* **2018**, *144*, 325-340. https://doi.org/10.1016/j.isprsjprs.2018.07.017

62. Zhao, F.; Feng, S.; Xie, F.; Zhu, S.; Zhang, S. Extraction of long time series wetland information based on Google Earth Engine and random forest algorithm for a plateau lake basin – A case study of Dianchi Lake, Yunnan Province, China. *Ecol. Indic.* **2023**,146,109813. doi: 10.1016/j.ecolind.2022.109813
63. Mohamed, A.; Abdelrady, M.; Alshehri, F.; Mohammed, M. A.; Abdelrady, A. Detection of Mineralization Zones Using Aeromagnetic Data. *Appl. Sci.* **2022**, 12, 9078, doi: 10.3390/app12189078
64. Grinand, C.; Rakotomalala, F.; Gond, V.; Vaudry, R.; M. Bernoux; Vieilledent, G. Estimating deforestation in tropical humid and dry forests in Madagascar from 2000 to 2010 using multidate Landsat satellite images and the random forests classifier. *Remote Sens. Environ.* **2013**, 139, 68-80. doi: 10.1016/j.rse.2013.07.008
65. Allouche, O.; Tsoar, A.; Kadmon, R. Assessing the accuracy of species distribution models: prevalence, kappa and the true skill statistic (TSS). *J. Appl. Ecol.* **2006**, 43, 1223-1232. doi: 10.1111/j.1365-2664.2006.01214.x
66. Schneider, A. Monitoring land cover change in urban and peri-urban areas using dense time stacks of Landsat satellite data and a data mining approach. *Remote Sens. Environ.* **2012**, 124, 689-704. doi: 10.1016/j.rse.2012.06.006
67. Weldegebriel, A.; Assefa, E.; Janusz, K.; Tekalign, M.; Van Rompaey, A. Spatial Analysis of Intra-Urban Land Use Dynamics in Sub-Saharan Africa: The Case of Addis Ababa (Ethiopia). *Urban Sci.* **2021**, 5, 57. doi: 10.3390/urbansci5030057
68. Orféo Toolbox. Change detection by Multivariate Alteration Detector (MAD) algorithm. Available online: https://www.orfeo-toolbox.org/CookBook-7.0/Applications/app_MultivariateAlterationDetector.html (accessed on 07 September 2024).
69. Ozcan, O.; Aksu, G. A.; Erten, E.; Musaoglu, N.; Cetin, M. Degradation monitoring in Silvo-pastoral systems: A case study of the Mediterranean region of Turkey. *Adv. Space Res.* **2019**, 63, 160-171. doi: 10.1016/j.asr.2018.09.009
70. INSEED. Deuxième Recensement Général de la Population et de l'Habitat (RGPH, 2). République du Tchad, 2009. Available online: https://unstats.un.org/unsd/demographic/sources/census/wphc/Chad/Chad_Resultats%20Globaux.pdf (Accessed on 04 September 20024).
71. Combary, Y. E. F.; Zemo, M. A. T.; Hemchi, H. M.; Atchrimi, B. T. Monitoring and assessing of sustainable development in the urban area of Ouagadougou based on SDG 11.3.1 indicator and the city biodiversity index. *Edelweiss Appl. Sci. Technol.* **2024**, 8, 1930-1943. doi: 10.55214/25768484.v8i6.2363
72. Sondou, T.; Anoumou, K. R; Aholou, C. C.; Chenal, J.; Pessoa Colombo, V. Urban Growth and Land Artificialization in Secondary African Cities: A Spatiotemporal Analysis of Ho (Ghana) and Kpalimé (Togo). *Urban Sci.* **2024**, 8, 207. doi: 10.3390/urbansci8040207
73. UNSD. SDG Indicator metadata. : https://unstats.un.org/sdgs/metadata/files/Metadata-11-03-01.pdf. Available online: https://sdg.data.gov/11-3-1/ (accessed on 15 November 2024).
74. U.S. SDG. Indicator 11.3.1 Ratio of land consumption rate to population growth rate. Available online: https://sdg.data.gov/11-3-1/ (accessed on 15 November 2024).
75. AL-Taani, A.; Al-husban, Y.; Farhan, I. Land suitability evaluation for agricultural use using GIS and remote sensing techniques: The case study of Ma'an Governorate, Jordan. *Egypt. J. Remote Sens. Space Sci.* **2021**, 24, 109-117. doi: 10.1016/j.ejrs.2020.01.001
76. Munyati, C. ; Drummond, J. H. Loss of urban green spaces in Mafikeng, South Africa. *World Dev. Perspect.* **2020**, 19,100226. doi: 10.1016/j.wdp.2020.100226

77. Enoguanbhor, E. C. ; Gollnow, F.; Nielsen, J. O.; Lakes, T. ; Walker, B. B. Land Cover Change in the Abuja City-Region, Nigeria: Integrating GIS and Remotely Sensed Data to Support Land Use Planning. *Sustainability* **2019**, 11, 1313. doi: 10.3390/su11051313
78. Dieng, M.A.; Keita, M. Télédétection et SIG dans l'analyse spatio-temporelle de la dynamique urbaine de Dakar, Sénégal. *Afrique SCIENCE* **2017**, 13, 292-306.
79. Mawenda, J.; Watanabe, T.; Avtar, R. An Analysis of Urban Land Use/Land Cover Changes in Blantyre City, Southern Malawi (1994–2018). *Sustainability* **2020**, 12, 2377. doi: 10.3390/su12062377
80. Mostafa, W.; Magd, Z.; Abo Khashaba, S. M.; Abdelaziz, B.; Hendawy, E.; Elfadaly, A.; Nabil, M.; Kucher, D. E.; Chen, S.; Mohamed, E. S. Impacts of Human Activities on Urban Sprawl and Land Surface Temperature in Rural Areas, a Case Study of El-Reyad District, Kafrelsheikh Governorate, Egypt. *Sustainability* **2023** 15,13497. https://doi.org/10.3390/su151813497
81. Chmielewski, J.; Kusztal, P.; Żeber-Dzikowska, I. Anthropogenic Impact on the Environment (Case Study). *Ochr. Srodowiska Zasobów Nat.* **2018**, 29, 30-37. doi: 10.2478/oszn-2018-0006
82. Mohamed, A.; Worku, H.; Lika, T. Urban and regional planning approaches for sustainable governance: The case of Addis Ababa and the surrounding area changing landscape. *City Environ. Interact.* **2020**, 8, 100050. doi: 10.1016/j.cacint.2020.100050